COMPUTATIONAL AEROSPACE ENGINEERING

ASSIGNMENT 3

Students: IVÁN SERMANOUKIAN MOLINA, YI QIANG JI ZHANG

Professor: JOAQUÍN ALBERTO HERNÁNDEZ ORTEGA

Aerospace Engineering
The School of Industrial, Aerospace and Audiovisual Engineering of Terrassa
Polytechnic University of Catalonia

January 20, 2021

Contents

1 Part 1 (basic)

1.1 Statement

Consider the cantilever box beam depicted in Figure 1. The length of the beam is $L_X = 2m$, its width and height $h_y = h_z = 0.25$ m, and its thickness $e = 0.05$ m. The material is isotropic, with $E = 70 \cdot 10^6 \mathrm{kN/m^2}$, and $\nu = 0.3$. The beam is subjected to a uniformly distributed load of value $t^{(2)} = -500 \mathrm{kN/m^2}$ on its top surface ($y = y_{\max}$)

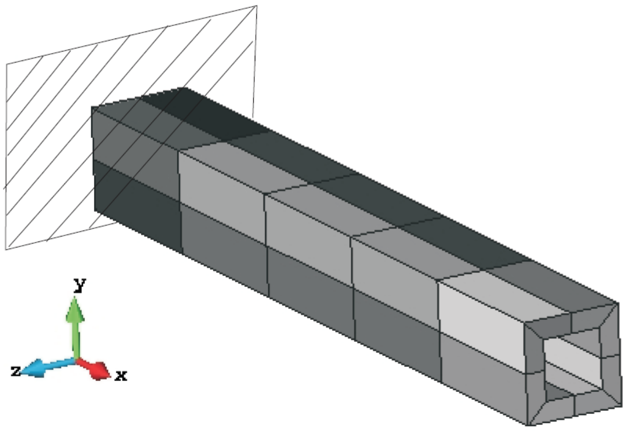

Figure 1 Cantilever box beam

Assess the convergence upon mesh refinement, by launching 4 different analyses with increasing number of finite elements (hexahedral). In particular, use semi-structured meshes with:

- MESH 1: $n_{ex} = 2$ divisions in the x -direction, and typical size in the $y - z$ plane of 0.1 m.
- MESH 2: $n_{ex} = 10$ divisions in the x -direction, and typical size in the $y - z$ plane of 0.05 m.
- MESH 3: $n_{ex} = 15$ divisions in the x -direction, and typical size in the $y - z$ plane of 0.05 m.
- MESH 4: $n_{ex} = 20$ divisions in the x -direction, and typical size in the $y - z$ plane of 0.025 m.

For these four cases, plot the distribution of vertical displacements (in the y-direction) along one of the edges on the top surface (parallel to the x-axis). Check also whether the maximum displacement at the tip of the beam converges to the analytical predictions provided by the theory of Strength of Materials.

2. Once the performance of the code has been properly assessed, study, for MESH 4, the finite element solution corresponding to the load state in which a torque T = 100kNm is applied at the free end (see figure below). HINT: replace this point torque by any statically equivalent system of point/distributed forces.

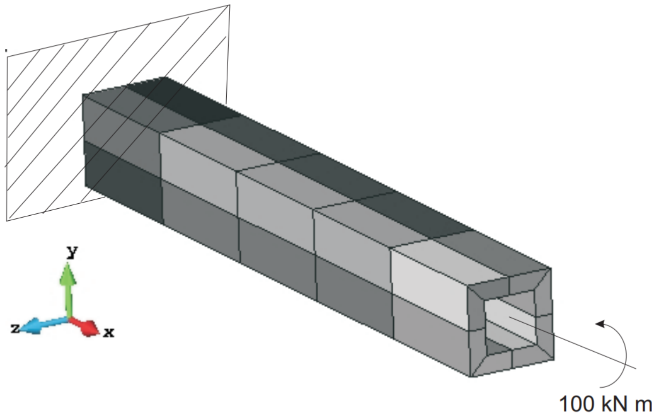

Figure 2 Cantilever box beam with a 100kNm torque

3. Code a matlab routine able to automatically compute the resultant of the reaction forces at the fixed end (R_x, R_y, R_z as well as M_x, M_y and M_z). Check that such reactions are in equilibrium with the prescribed forces.

1.2 Resolution

1.2.1 Displacement study

The results obtained from the numerical simulation using GID in order to obtain the vertical displacements along the top edge are plotted as follows:

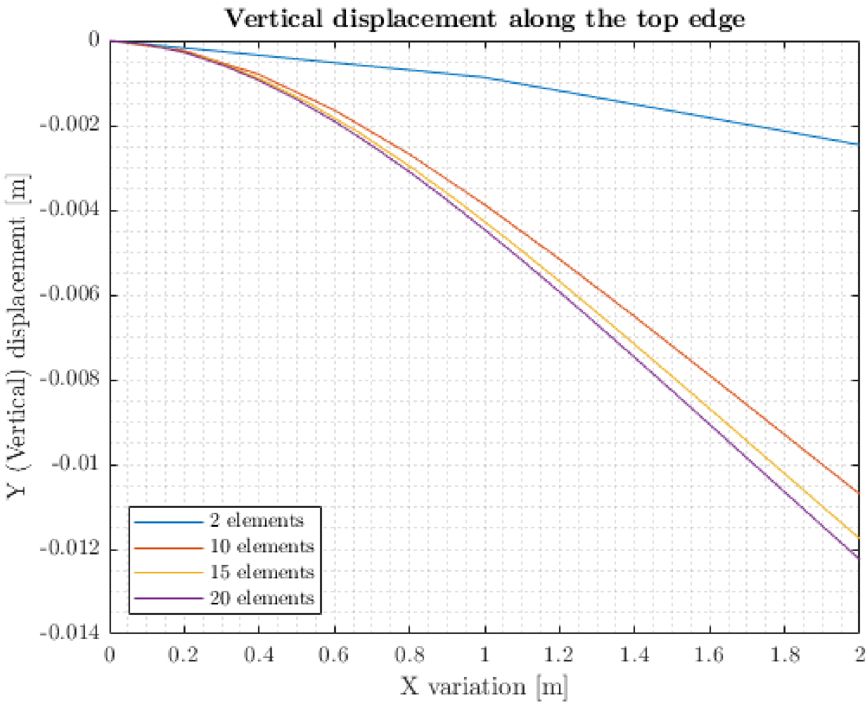

Figure 3 Vertical displacement along the top edge

The verification of the maximum displacement at the tip convergence to the analytical prediction is provided by the theory of Strength of Materials. Thus, the cantilever beam equation subjected to a uniformly distributed load will be used:

$$\delta_t = \frac{q \cdot L^4}{8EI_z} \tag{1}$$

where L is the bar longitude and E corresponds to the Young modulus, both constant with a known value. Then, the distributed load q has to be transformed in order to suit the problem data, which states that the provided value is the load per unit of surface while Eq.1 considers a load per unit of length. As a result, the following alteration is considered:

$$q = t^{(2)} \cdot h_z \tag{2}$$

where $t^{(2)}$ corresponds to the load per unit of surface and h_z is the width of the bar on the z axis.

Substituting the given values, the theory of Strength of Materials states that q would be:

$$q = -125kN/m \tag{3}$$

Subsequently, the only geometrical parameter that is needed is the second moment of area along the z-direction I_z apart from the bar's longitude L. To obtain this parameter, we can consider the subtraction of the moment of inertia of the outer section $[h_z \cdot h_y]$ and the internal square $[(h_z - e) \cdot (h_y - e)]$:

$$I_z = \underbrace{\left[\frac{1}{12} \cdot (h_y)^3 \cdot h_z\right]}_{\text{Outer square}} - \underbrace{\left[\frac{1}{12} \cdot (h_y - 2e)^3 \cdot (h_z - 2e)\right]}_{\text{Inner square}} \tag{4}$$

Replacing the values,

$$I_z = \underbrace{\left[\frac{1}{12} \cdot (0.25)^3 \cdot 0.25\right]}_{\text{Outer square}} - \underbrace{\left[\frac{1}{12} \cdot (0.25 - 2 \cdot 0.05)^3 \cdot (0.25 - 2 \cdot 0.05)\right]}_{\text{Inner square}} = 2.83333 \cdot 10^{-4} \text{ m}^4 \tag{5}$$

With the value of I_z the vertical displacement using Eq. 1 is:

$$d = -0.012605\, m \tag{6}$$

If this value is compared with those from Fig. 3, the following results are obtained:

Mesh	**Number of elements (longitudinal axis X)**	**Maximum displacement [m]**	**% of error with theoretical value**
1	2	-0.00246	80.49
2	10	-0.01070	15.15
3	15	-0.01176	6.74
4	20	-0.01225	2.85

Table 1 Numerical results using Finite Element Method

As it can be seen, the values converge to the theoretical demonstration while diminishing the percentage of error. If more elements were used, the values would be closer to the theoretical analysis but would not change significantly so it is considered that the mesh with 20 elements yields appropriate results.

Notice that the negative sign of the displacement indicates that the deformed structure is deformed with respect to the negative direction of y axis. The maximum displacement occurs at $x = L$, both theoretical and finite element method values are quite similar. Indeed, increasing the size of the elements shows a more precise values of displacements. For instance, considering 20 elements, the error between the FEM and the theoretical one is over 2%, which in fact, confirms the convergence of the results.

Additional, the displacement at the root of the bar is exactly 0, which means that the structure does not move in any direction at the root. Thereby, this implies that initial Dirichlet conditions are well defined and imposed.

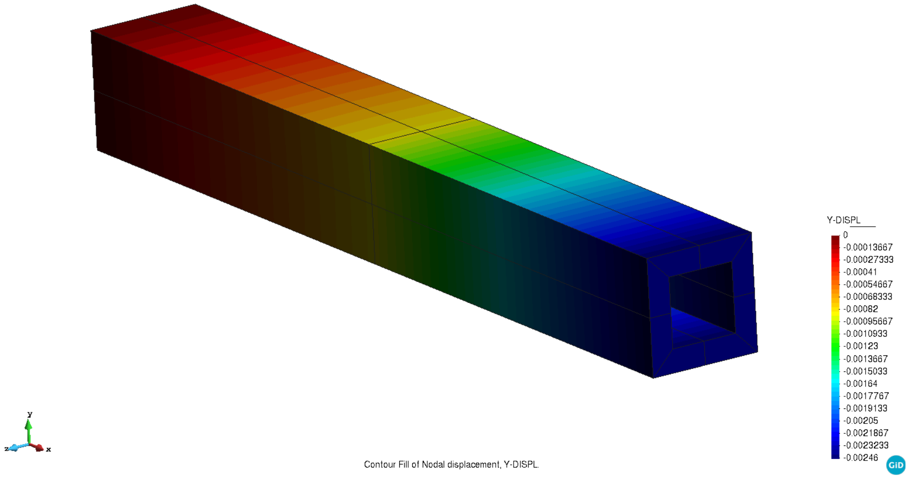

(a) $n_{el} = 2$ element

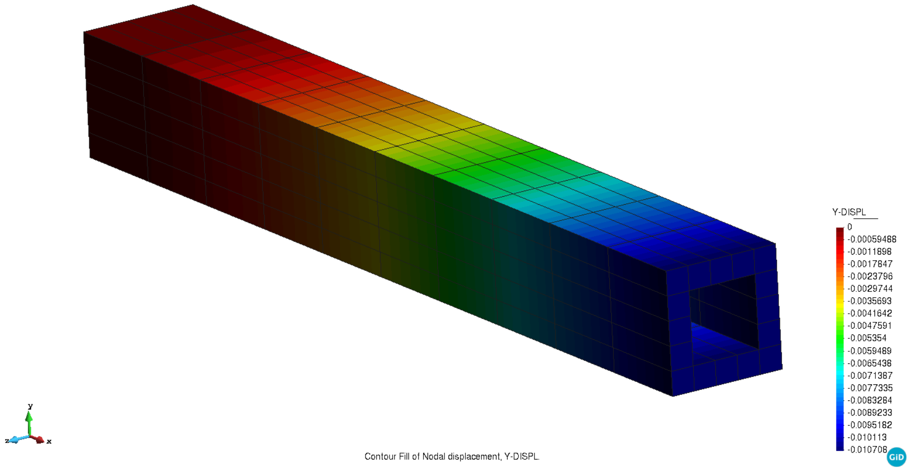

(b) $n_{el} = 10$ elements

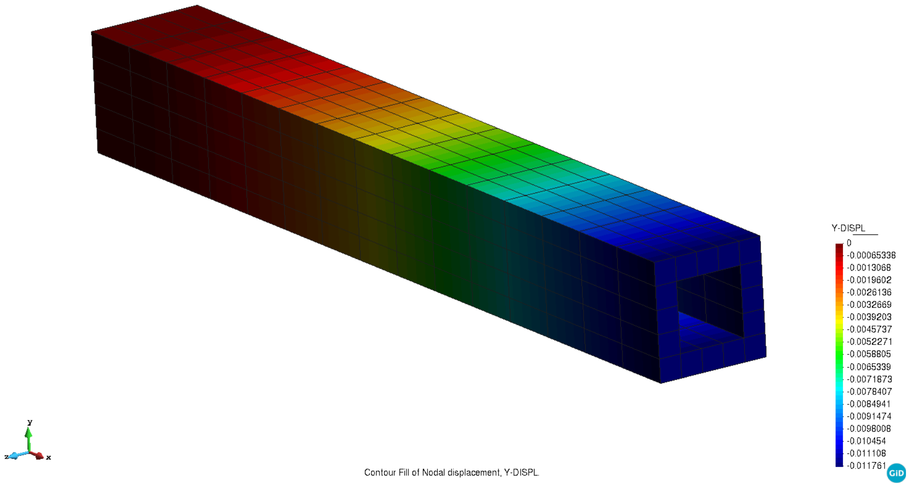

(c) $n_{el} = 15$ elements

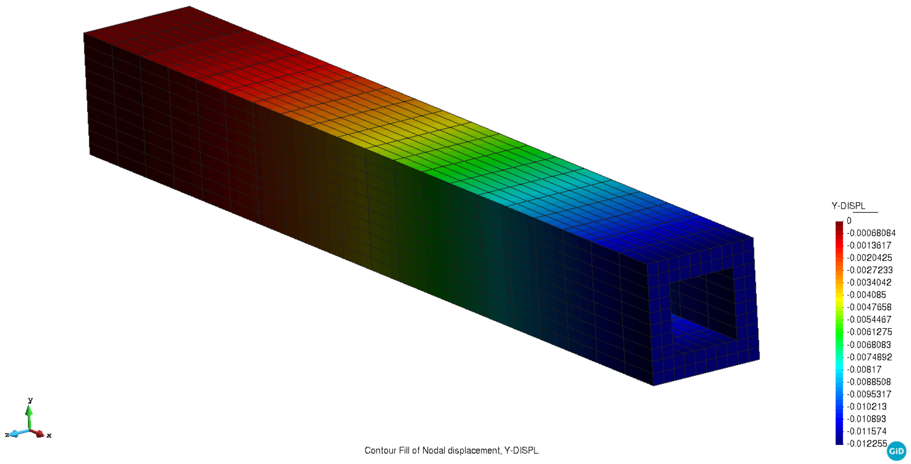

(d) $n_{el} = 20$ elements

Figure 4 Vertical displacements for all elements

1.2.2 Bending moment study

The figure below shows a the diagram view of the cross section (see Figure 5) and longitudinal section (see Figure 6) of the beam structure.

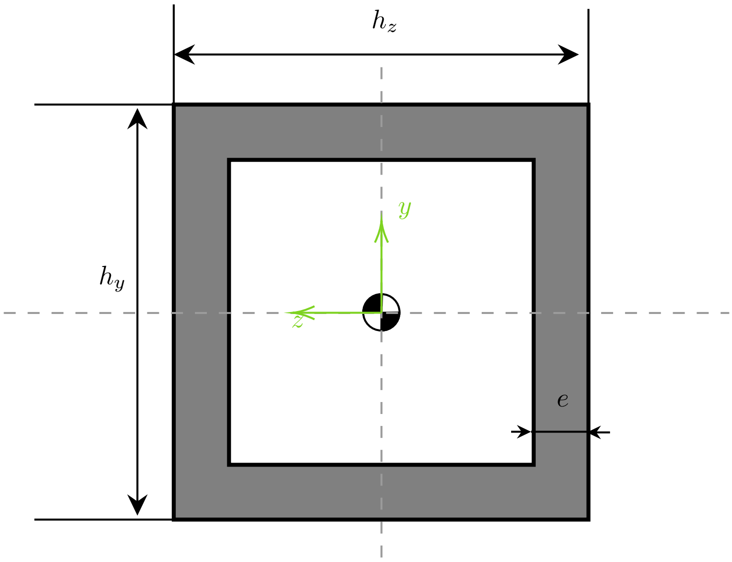

Figure 5 Cross section view

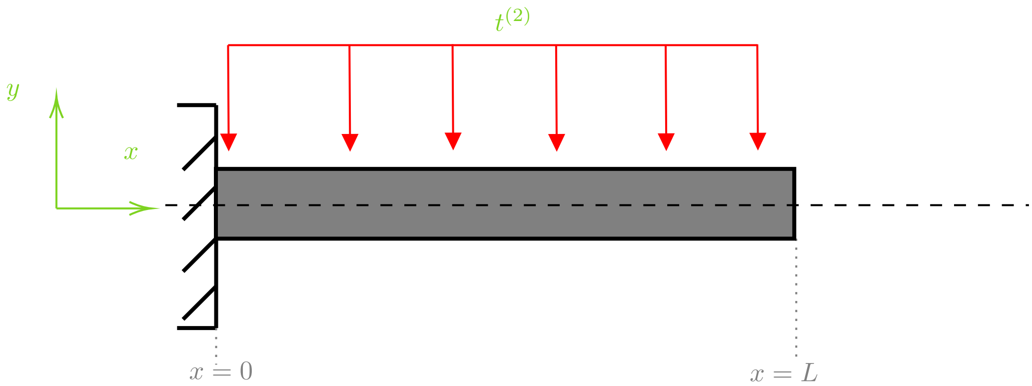

Figure 6 Longitudinal section view

As the beam's longitude $L = 2$ m is much larger than its thickness $e = 0.05$ m, the theory of thin-beams can be used to calculate the reaction stresses and forces. Thus, using Navier-Bernoulli's expression in compliance with the coordinate axis, the expression of the stress considering the central fiber and the centroid is the following:

$$\sigma = \frac{N}{A} - \frac{M_z}{I_z}y + \frac{M_y}{I_y}z \tag{7}$$

The Navier-Bernouilli equation components are explained below:

- σ: Represents the normal stress at any given point.
- N: Is the axial force applied to the beam (In particular, this problem has $N = 0$).
- M_z: z axis bending moment.
- M_y: y axis bending moment.

- I_z: z axis second moment of area.
- I_y: y axis second moment of area.

The expression above considers the symmetry of the structure, which implies that all products of inertia ($I_{yz} = I_{zy} = 0$). Also, for any unsymmetrical cross-section, there exists a centroidal set of axes for which the product of second moment of area is zero.

Particularizing the set of equations to our problem, there is not any force or torque applied in the x and since the only force applied to the structure is the distributed force in the y axis (t^2), the first and latter term are null. Thereby, the expression is reduced to:

$$\sigma = -\frac{M_z}{I_z} y \tag{8}$$

Eventually, the maximum bending moment will occur at the root of the structure. Intuitively, the structure will bend with a $M_z < 0$. If we get the Neutral Fiber equation by equaling the Navier-Bernouilli equation to 0:

$$\sigma = -\frac{M_z}{I_z} y = 0 \quad \longrightarrow \quad y = 0 \tag{9}$$

This means that the neutral fiber is located in the z axis. Thereafter, once the neutral fiber is known, it is simple to see that the most solicited fiber is the furthest point with respect to the z axis, thus, $y = \frac{h_y}{2}$. Consequently, the stress at that point can be computed as

$$\sigma_{max} = -\frac{t^{(2)} \cdot L_z \cdot h_z \cdot \frac{L}{2}}{I_z} y = -1.102941 \cdot 10^8 \text{ Pa} \tag{10}$$

1.2.3 Torque study

This part of the problem consists of studying the $M_x = 100$ kN torque applied to the structure. Below is presented the structure of the mesh and the point forces (see Figure 7 and 7).

Theoretically, it is not possible to introduce a torque to the Finite Element Method program. Nonetheless, a torque can be thought of a point force acting on a set of specific nodes that generates the same torque as the additional torque of $M_x = 100$ kN. To do so, we translate the torque into a point force, for the sake of simplicity, the analogous point forces were set to specific nodes in the center line.

Considering the mesh with 20 (hexaedral finite elements), two different options have been implemented. The first one considers 2 point forces of 0.25 MN in at nodes 31 and 161. On the other hand, if 4 forces are considered, 2 additional nodes are added up and bottom at nodes 35 and 163.

$$T = F \cdot d \tag{11}$$

- **Case with 2 point forces**:

$$100 \text{ kN} = 2 \cdot F_{\text{equivalent}} \cdot \frac{h_z}{2} - \frac{e}{2} \quad \longrightarrow \quad F_{\text{equivalent}} = 0.5 \text{ MN} \tag{12}$$

- **Case with 4 point forces**:

$$100 \text{ kN} = 4 \cdot F_{\text{equivalent}} \cdot \frac{h_z}{2} - \frac{e}{2} \quad \longrightarrow \quad F_{\text{equivalent}} = 0.25 \text{ MN} \tag{13}$$

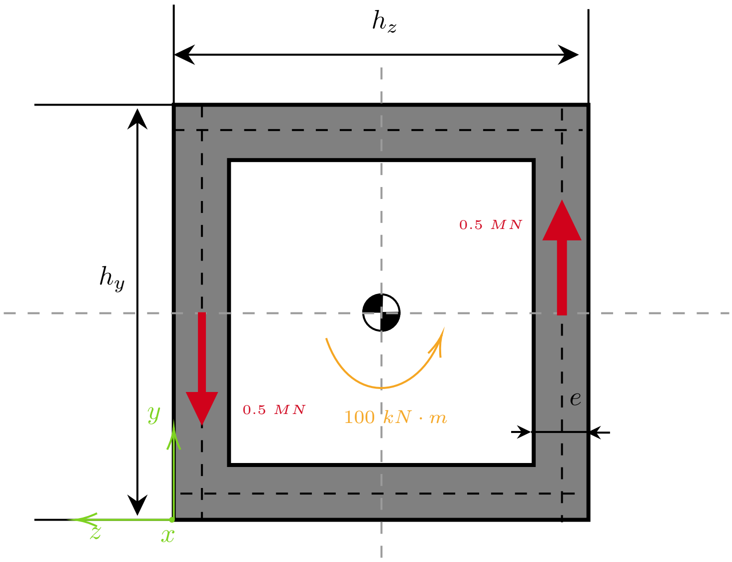

Figure 7 Torque analogy with 2 point forces

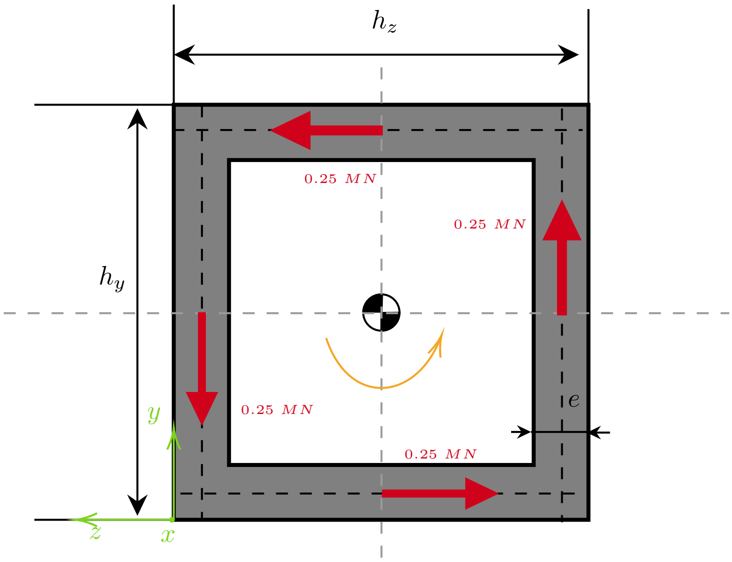

Figure 8 Torque analogy with 4 point forces

1.2.3.1 Y-axis displacement

Subsequently, the distribution of nodal displacements in the y axis are presented below (see Figure 9 and Figure 12).

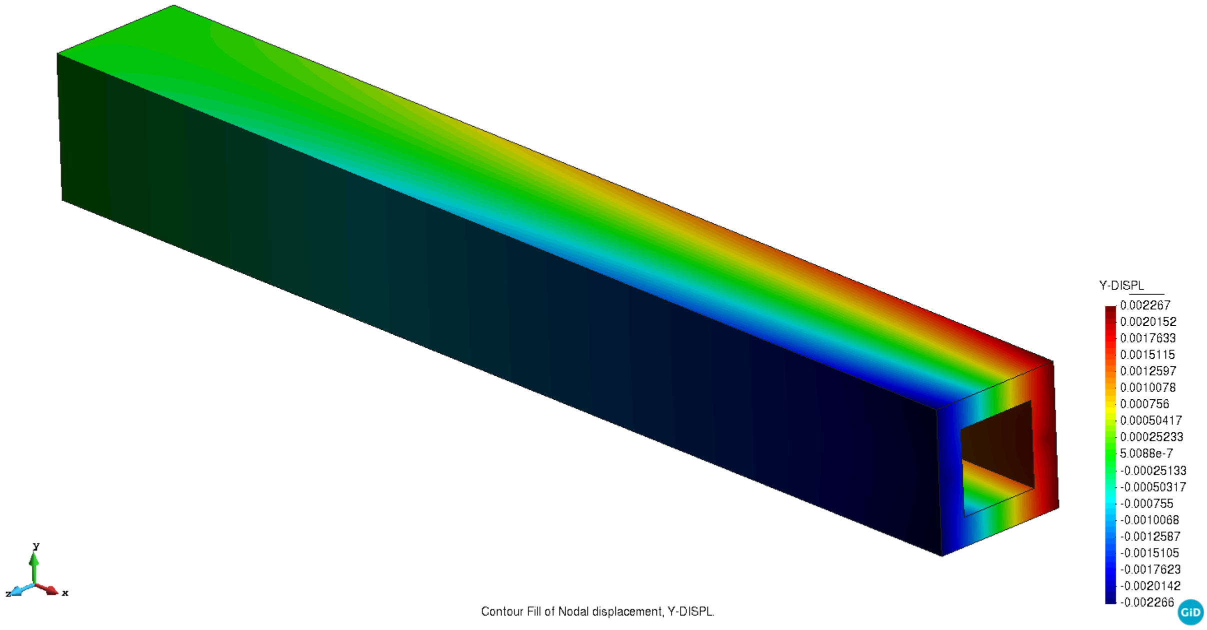

Figure 9 Displacement on the Y axis with 2 point forces

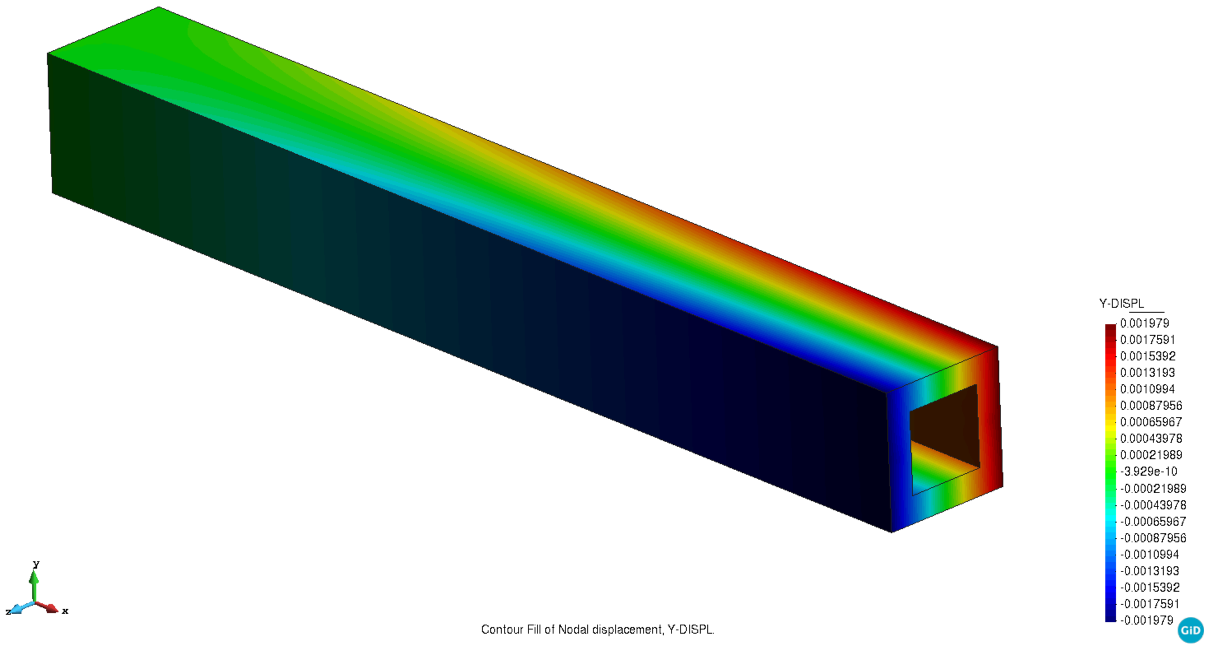

Figure 10 Displacement on the Y axis with 4 point forces

As shown in the post processed plots, both right hand side and left hand side of the beam with respect to y axis are the ones that suffers most. The distribution is symmetrical with respect to the xy plane. The right hand side nodes have a positive displacement along the y axis whereas the left hand side have a negative displacement.

1.2.3.2 Z-axis displacement

Plotting the results for the displacement along the z axis, the tendency is the same as the y axis displacement. The above nodes moves in the positive direction with the z axis direction whereas the bottom part is moves towards the negative direction of the z axis.

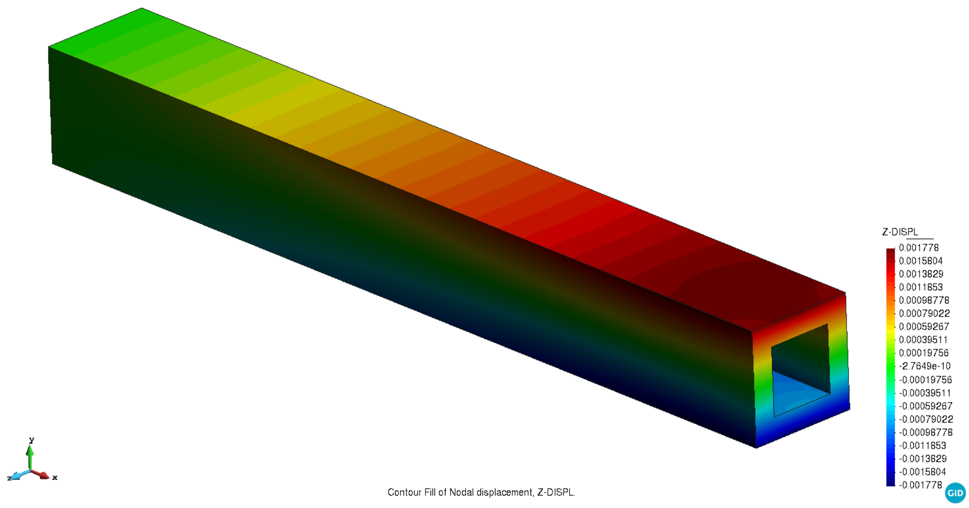

Figure 11 Displacement on the Z axis with 2 point forces

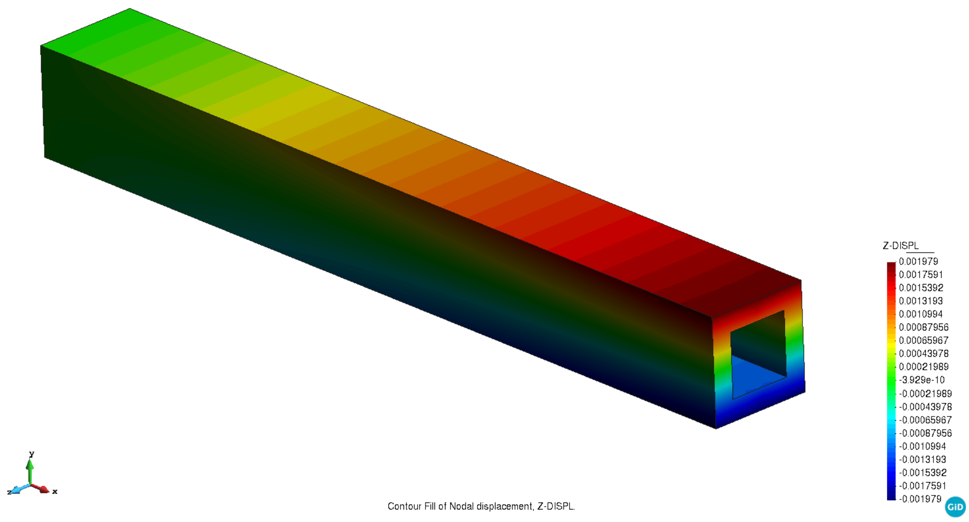

Figure 12 Displacement on the Z axis with 4 point forces

1.2.3.3 Total displacements

Finally, summing up both displacements contributions, the final displacement is shown below in figures 13 and 14. The resultant displacement follows the logical direction following the direction of the torque variation. It is important to mention that the effect along the structure is diminished since the nodes at $x = 0$ are set to have no displacement (Dirichlet condition). Notice how the free ends have the most importance displacement.

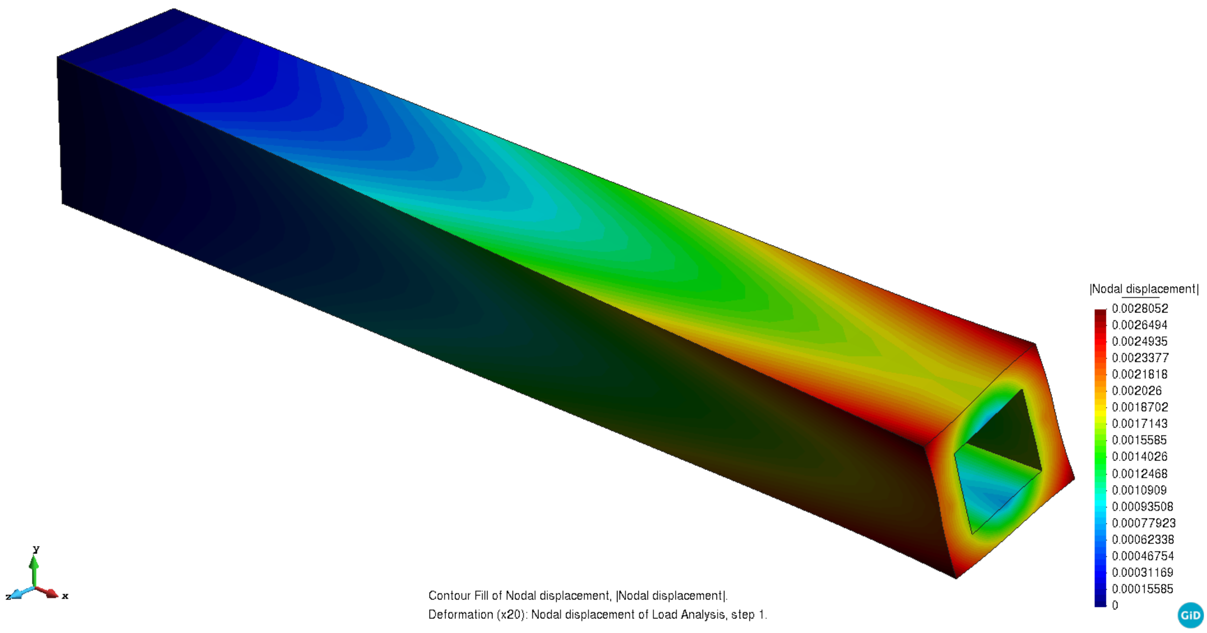

Figure 13 Total displacements with 2 point forces

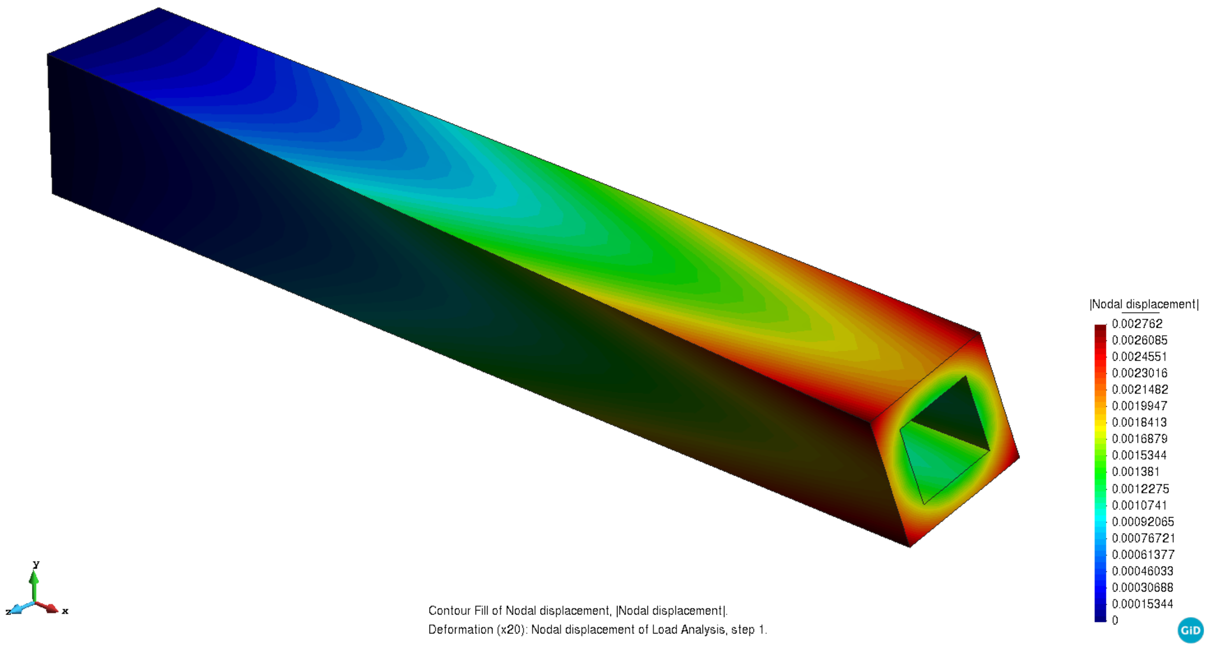

Figure 14 Total with 4 point forces

1.2.4 Reaction forces and torques

Calculating the reaction forces and torques for each mesh yield the following results:

Mesh	Number of elements (longitudinal axis X)	Rx [MN]	Ry [MN]	Rz [MN]
1	2	$2.2760 \cdot 10^{-15} \approx 0$	0.25	$-1.4391 \cdot 10^{-14} = \approx 0$
2	10	$-1.6487 \cdot 10^{-14} \approx 0$	0.25	$8.5931 \cdot 10^{-14} \approx 0$
3	15	$2.0914 \cdot 10^{-14} \approx 0$	0.25	$2.7277 \cdot 10^{-14} \approx 0$
4	20	$-1.4988 \cdot 10^{-14} \approx 0$	0.25	$-2.1474 \cdot 10^{-13} \approx 0$
5	20 (+torque)	$6.03467 \cdot 10^{-15} \approx 0$	$-9.6406 \cdot 10^{-14} \approx 0$	$-8.5990 \cdot 10^{-15} \approx 0$

Mesh	Number of elements (longitudinal axis X)	Mx [MNm]	My [MNm]	Mz [MNm]
1	2	$-5.9219 \cdot 10^{-15} \approx 0$	$1.2608 \cdot 10^{-14} \approx 0$	0.25
2	10	$-1.7385 \cdot 10^{-14} \approx 0$	$-1.5554 \cdot 10^{-13} \approx 0$	0.25
3	15	$-2.4321 \cdot 10^{-15} \approx 0$	$-2.7282 \cdot 10^{-14} \approx 0$	0.25
4	20	$6.4304 \cdot 10^{-14} \approx 0$	$2.71384 \cdot 10^{-13} \approx 0$	0.25
5	20 (+torque)	-0.10	$6.2518 \cdot 10^{-15} \approx 0$	$-1.2197 \cdot 10^{-13} \approx 0$

Considering the fourth mesh with 20 elements but without an external torque, the equilibrium can be checked. Considering the analog system with a punctual force:

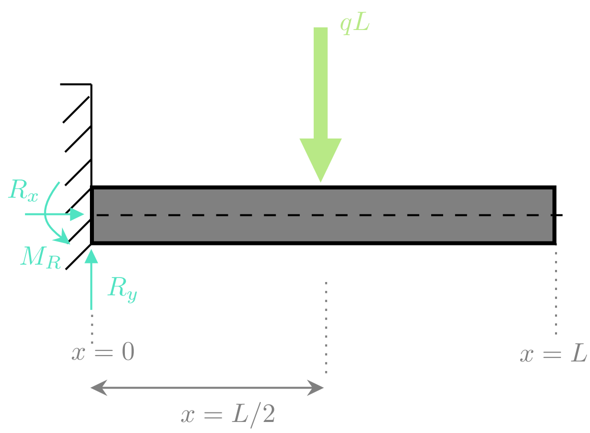

Figure 15 Analog diagram of the forces and moments on the beam

As no external forces are applied on the first case along both x and z axis, the corresponding reactions are null:

$$\sum Fx = 0 \quad \longrightarrow \quad R_x = 0 \tag{14}$$

$$\sum Fy = 0 \quad \longrightarrow \quad R_y - qL = 0 \quad \longrightarrow \quad R_y = qL \tag{15}$$

$$\sum Fz = 0 \quad \longrightarrow \quad R_z = 0 \tag{16}$$

And the same has to happen with the moments:

$$\sum M_x = 0 \quad \longrightarrow \quad M_x = 0 \tag{17}$$

$$\sum M_y = 0 \quad \longrightarrow \quad M_y = 0 \tag{18}$$

$$\sum Mz = 0 \quad \longrightarrow \quad M_z - qL \cdot \frac{L}{2} = 0 \quad \longrightarrow \quad M_z = qL \cdot \frac{L}{2} \tag{19}$$

As a result, the reactions are in equilibrium.

2 Part 2 (advanced)

2.1 Thermoelasticity

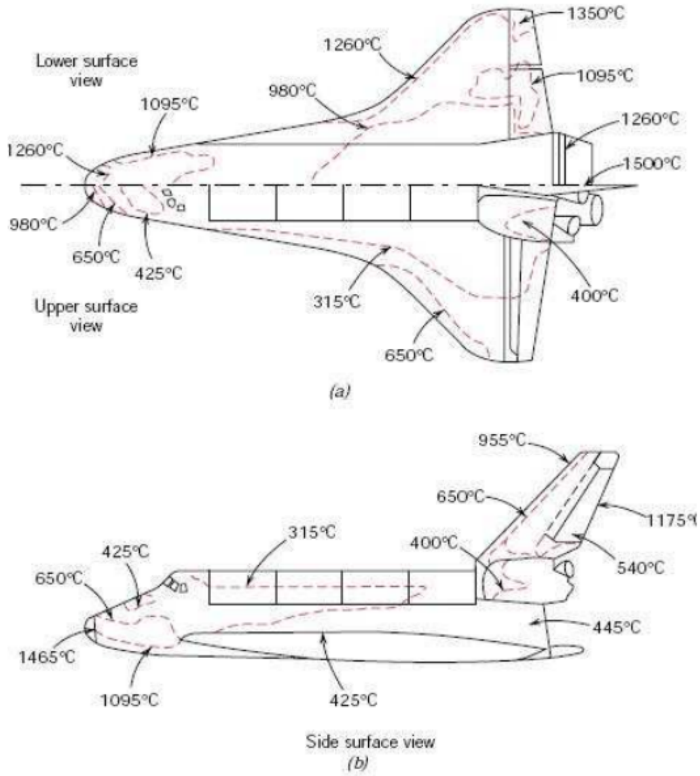

Figure 16 Approximate maximum outer surface temperature profiles for the Space Shuttle Orbiter during reentry: (a) upper and lower views; (b) side view.

It is well-known that changes of temperature in elastic bodies produce strains. In the linear regime, such strains are calculated by

$$\varepsilon_{ij}^{\text{thermal}} = \alpha_{ij} \Delta T$$

where α_{ij} denotes the tensor of thermal expansion coefficients ($i, j = 1, 2, 3$ for 3D problems), while $\Delta T = T - T_0$ represents the variation of temperature with respect to the reference temperature $T_0 = T_0(\boldsymbol{x})$ In isotropic materials, α_{ij} can be expressed by

$$\boldsymbol{\alpha} = \alpha \begin{bmatrix} 1 & 0 & 0 \\ 0 & 1 & 0 \\ 0 & 0 & 1 \end{bmatrix}$$

In Voigt notation, the preceding expressions adopt the form

$$\varepsilon^{\text{thermal}} = \boldsymbol{\alpha} \Delta T$$

where

$$\boldsymbol{\alpha} = \begin{bmatrix} 1 \\ 1 \\ 1 \\ 0 \\ 0 \\ 0 \end{bmatrix}$$

2.2 Thermo-mechanical constitutive equation

The weak statement of the boundary value equilibrium problem reads (see page 30 of the theory document

$$\text{W.F.} \quad \begin{cases} \text{Given } f : \Omega \to R^{n,d}, \bar{t} : \Gamma_\sigma \to R^{n,d}, \text{ find } u \in \mathcal{S} \text{ such that} \\ \displaystyle\int_\Omega \nabla^s v^T \sigma d\Omega = \int_\Omega v^T f d\Omega + \int_{\Gamma_\sigma} v^T \bar{t} d\Gamma \quad \forall v \in \mathcal{V} \end{cases} \tag{20}$$

In the isothermal case, we know that $\sigma = C\nabla^n u$, that is, the stresses depend exclusively on the symmetric gradient of the displacements. To account for thermal effects, it is necessary to modify this constitutive equation and introduce the thermal strains defined in Eq.(2.3). This is done as follows (see e.g. Reference [2]):

$$\nabla^n u = C^{-1}\sigma + \alpha \Delta T$$

By solving this equation for $\boldsymbol{\sigma}$, we obtain the desired constitutive equation

$$\boldsymbol{\sigma} = \boldsymbol{C}\left(\nabla^s \boldsymbol{u} - \boldsymbol{\alpha}\Delta T\right) = \boldsymbol{C}\nabla^s \boldsymbol{u} - \boldsymbol{\beta}\Delta T$$

where

$$\boldsymbol{\beta} := \boldsymbol{C}\boldsymbol{\alpha}$$

For an isotropic material, we have that

$$\boldsymbol{\beta} = \boldsymbol{C}\boldsymbol{\alpha} = \begin{bmatrix} \lambda + 2\mu & \lambda & \lambda & 0 & 0 & 0 \\ \lambda & \lambda + 2\mu & \lambda & 0 & 0 & 0 \\ \lambda & \lambda & \lambda + 2\mu & 0 & 0 & 0 \\ 0 & 0 & 0 & \mu & 0 & 0 \\ 0 & 0 & 0 & 0 & \mu & 0 \\ 0 & 0 & 0 & 0 & 0 & \mu \end{bmatrix} \begin{bmatrix} \alpha \\ \alpha \\ \alpha \\ 0 \\ 0 \\ 0 \end{bmatrix} = \kappa\alpha \begin{bmatrix} 1 \\ 1 \\ 1 \\ 0 \\ 0 \\ 0 \end{bmatrix}$$

where κ stands for the bulk modulus of the material.

$$\kappa := 3\lambda + 2\mu = 3\frac{\nu E}{(1+\nu)(1-2\nu)} + 2\frac{E}{2(1+\nu)} = \frac{E}{1-2\nu}$$

2.3 Requested tasks

2.3.1 Derivation of thermo-mechanical equilibrium equations

Let $\Omega = \cup_{e=1}^{n_d} \Omega^c$ be a given finite element discretization. Suppose we solve the heat conduction problem explained in chapter 2 under given boundary conditions, and obtains the vector of temperatures, $\boldsymbol{\theta}$, at the nodes of the discretization (with respect to the reference temperature T_0). With this vector at our disposal, we can interpolate the relative temperature at any point within an element Ω^c by the corresponding shape functions:

$$\Delta T(\boldsymbol{x}) = \mathcal{N}^2(\boldsymbol{x})\boldsymbol{\theta}^e, \quad \boldsymbol{x} \in \Omega^e$$

where θ^- denotes the vector of nodal temperatures of element Ω^*. With this consideration in mind, derive the discrete system of equilibrium equations arising from the variational principle (2.5) when the stresses depend on the temperature through equation (2.7)

- HINT: The contribution of the temperature to the final system of equation is a vector of "thermal forces": $\boldsymbol{F}_{th}$, similar to that of, for instance, the body forces, in the sense that it can be obtained by assembly of element contributions $\boldsymbol{F}^e_{th}$. The student is requested to show how to obtain the element vector $\boldsymbol{F}^e_{th}$ as a function of $\boldsymbol{\theta}^c$ using the variational formulation (2.5)

2.4 Resolution

Recalling the weak form of the problem, the first step is to substitute the constitutive equation with the variational formulation of the mechanical problem.

Recalling the strong form of the heat dependent transfer problem, we are going top formulate it by means of the variational or weak form.

$$\int_\Omega v(\nabla q - f)\ \mathrm{d}\Omega = \int_\Omega v\left(\rho c \frac{\partial u}{\partial t}\right)\ \mathrm{d}\Omega \tag{21}$$

Developing the expression according to the theory given in class, it results in the following expression:

$$-\int_\Omega (\nabla)\cdot q\ \mathrm{d}\Omega = \int_\Gamma v(-q)\ \mathrm{d}\Gamma - \int_\Gamma vf\ \mathrm{f}\omega = \int_\Omega v\left(\rho c \frac{\partial u}{\partial t}\right)\ \mathrm{d}\Omega \tag{22}$$

Rearranging the above expression, the variational weak formulation is the following:

$$\int_\Omega v\left(\rho c \frac{\partial u}{\partial t}\right)\ \mathrm{d}\Omega \tag{23}$$

Once the variational formulation is reached, applying the definitions for space and spatial formulation and adding the time derivative for the trial function we finally can get the problem by its matrix format:

$$\frac{\partial u}{\partial t} = \frac{\partial (Nd)}{\partial t} = N\frac{\partial d}{\partial t} + d\frac{\partial N}{\partial t} \tag{24}$$

Since the shape functions are not time dependant, they are functions of space dimension. The latter term of the above expression can be written as

$$\frac{\partial u}{\partial t} = \frac{\partial (Nd)}{\partial t} = N\frac{\partial d}{\partial t} = Nd \tag{25}$$

Defining trial and test functions and its derivatives, the expression above can be rewritten as follows:

$$u = \mathbf{N}\cdot d \tag{26}$$

$$v = \mathbf{N}\cdot c = c^T N^T \tag{27}$$

$$\nabla u = \mathbf{B}\cdot d \tag{28}$$

$$\nabla v = \mathbf{B}\cdot c = c^T B^T \tag{29}$$

$$\mathbf{B} = \nabla\mathbf{N} \tag{30}$$

Finally, introducing the corresponding trial and test functions into the variational form

$$c^T\left[\left(\int_\Omega N^T \rho c N\ \mathrm{d}\Omega\right)\dot{d} - \left(\int_\Omega (B^T\cdot\kappa\cdot B\mathrm{d}\Omega\right)\cdot d + c^T\left(\int_\Omega N^T\cdot f\mathrm{d}\Omega + \int_{\Gamma_b} N^T\cdot f\ \mathrm{d}\Omega + \int_{\Gamma_b} N^T q\mathrm{d}\Gamma\right)\right] \tag{31}$$

The input function $\bar{t}$ can be replaced by the interpolation of the boundary test functions.

$$F^e_{tdis} = \int_{\Gamma^e_b} \overline{N}^{eT}\bar{t}\ \mathrm{d}\Gamma \tag{32}$$

Where t^e represents the vector containing the values of the function $\bar{t}$ at each node of the boundary element e.

$$F^e_{tdis} = \int_{\Gamma^e_b} \overline{N}^{eT} (N^e \bar{t}^e) \, \mathrm{d}\Gamma \tag{33}$$

Finally, for the traction vector, the can be computed as:

$$F_{tdis} = \sum_{e \in E_b} \overline{L}^{eT} F^e_{tdis} \tag{34}$$

However, there is an additional "thermal force" that needs to be accounted. It is necessary to obtain the element thermal force vector as a function of the vector of nodal temperatures of the elements in which the domain has been discretized. Thereby,

$$F_{th} = \int_{\Omega} B^T \beta \Delta T \mathrm{d}\Omega \tag{35}$$

Developing the algebraic expression,

$$\nabla^s v^T \beta \Delta T \, \mathrm{d}\Omega \tag{36}$$

By replacing the previous expressions into the above equation we arrive at:

$$\sum_{e=1}^{n_{el}} e^{eT} \int_{\Omega^e} \nabla^s v^T \beta \Delta T \mathrm{d}\Omega \tag{37}$$

Next, we apply the relation based on the interpolation of the relative temperature at any point of the domain within an element Ω^e, we arrive at

$$\sum_{e=1}^{n_{el}} e^{eT} \int_{\Omega^e} B^{eT} \beta N^e \theta^e \mathrm{d}\Omega = \sum_{e=1}^{n_{el}} e^{eT} F^e_{th} \tag{38}$$

Thus, the elemental force vector, as a funtion of the nodal temperatures (θ^e) can be expressed as:

$$\boxed{F^e_{th} = \int_{\Omega^e} B^{eT} \beta N^e \theta^e \mathrm{d}\Omega} \tag{39}$$

Besides,

$$c^T \sum_{e=1}^{n_{el}} L^{eT} F_{th} \tag{40}$$

Then the global vector force is obtained by:

$$\boxed{F_{th} = \sum_{e=1}^{n_{el}} L^{eT} F^e_{th}} \tag{41}$$

References

[1] Hernández, Joaquín. "Classical Linear Elastostatics". In: 1st ed. UPC, 2020, pp. 1–106.